Environmental Modelling and Software 130 (2020) 104739

Contents lists available at ScienceDirect

Environmental Modelling and Software

journal homepage: http://www.elsevier.com/locate/envsoft

Introducing QWaterModel, a QGIS plugin for predicting evapotranspiration from land surface temperatures

Florian Ellsäßer [a,*], Alexander Röll [a], Christian Stiegler [b], Hendrayanto [c], Dirk Hölscher [a,d]

[a] University of Göttingen, Tropical Silviculture and Forest Ecology, Büsgenweg 1, 37077, Göttingen, Germany
[b] University of Göttingen, Bioclimatology, Büsgenweg 2, 37077 Göttingen, Germany
[c] Bogor Agricultural University, Forest Management, Campus Darmaga Bogor, Jawa Barat 16680, Indonesia
[d] University of Göttingen, Centre of Biodiversity and Sustainable Land Use (CBL), Büsgenweg 1, 37077, Göttingen, Germany

ARTICLE INFO

Keywords:
Evaporation
Transpiration
Water cycle
DATTUTDUT
Energy balance
Open source
Hydrological modeling
Thermography
Thermal images
Drone
UAV

ABSTRACT

Evapotranspiration (ET) is a central flux in the hydrological cycle. Various approaches to compute ET via energy balance models exist, but their handling is often complex and challenging. We developed QWaterModel as an easy-to-use tool to make ET predictions available to broader audiences. QWaterModel is based on the DATTUTDUT energy balance model and uses land surface temperature maps as an input. Such maps can e.g. be obtained from satellite, drone or handheld camera imagery. In the present study, we successfully tested QWaterModel for predicting ET in a tropical oil palm plantation against the well-established eddy covariance method. QWaterModel is compatible with all versions of QGIS3 and is available from the official QGIS Plugin Repository.

1. Introduction

Evapotranspiration (ET) is the combined water flux of evaporation from soil, plant and water surfaces as well as transpiration from plants (Allen et al., 1998). Terrestrial ET is a major flux in the hydrological cycle consuming about 60% of terrestrial precipitation (Oki and Kanae, 2006). Associated with climate and land-use change, major transformations in the global hydrological cycle are projected; therefore, a broad understanding and knowledge of ET and its patterns are of paramount importance (Kaushal et al., 2017; Ziegler et al., 2003). The current understanding of how ecosystems respond to such changes is limited by insufficient monitoring capabilities (Fisher et al., 2017). The development of effective adaption strategies for agriculture, ecosystems and water management will depend on the availability of ET assessment schemes that can be readily applied from local to global scales (Fisher et al., 2017). ET can be measured locally using e.g. the eddy covariance method or estimated at larger spatial scales by applying energy balance models. For many energy balance models remotely-sensed land surface temperatures (LST) are used as principal input, therein assuming that hot pixels are the result of low ET and cold pixels indicate high ET (Timmermans et al., 2015). Current developments such as increasing computation power, extensive availability of free satellite imagery (e.g. from Landsat 7 and 8) and a large variety of portable thermal cameras that can be attached to drones or used as handheld devices foster the use of energy balance modeling for ET estimation (Hoffmann et al., 2016; Maes and Steppe, 2012; Timmermans et al., 2015; Xia et al., 2016). However, most energy balance models are complex and their implementation requires advanced programming skills and technical expertise, which constitutes a barrier for the application of energy balance models for ET estimation.

To overcome this barrier, we developed the QGIS plugin 'QWaterModel', which addresses the following objectives: to facilitate the use of energy balance and evapotranspiration modeling, to take LST images and maps from a wide range of sources including satellites, planes, drones and handheld thermal cameras as input, to reduce the use of complementary data to a feasible level and to use a documented open source structure to encourage further development. In the present study, we explain and test key-features of QWaterModel in a scientific context, using exemplary LST data from different sources recorded in an oil palm plantation in Indonesia to compute ET estimates. We then compare the

* Corresponding author.
E-mail address: fellsae@gwdg.de (F. Ellsäßer).

https://doi.org/10.1016/j.envsoft.2020.104739
Received 2 April 2020; Received in revised form 13 May 2020; Accepted 13 May 2020
Available online 18 May 2020

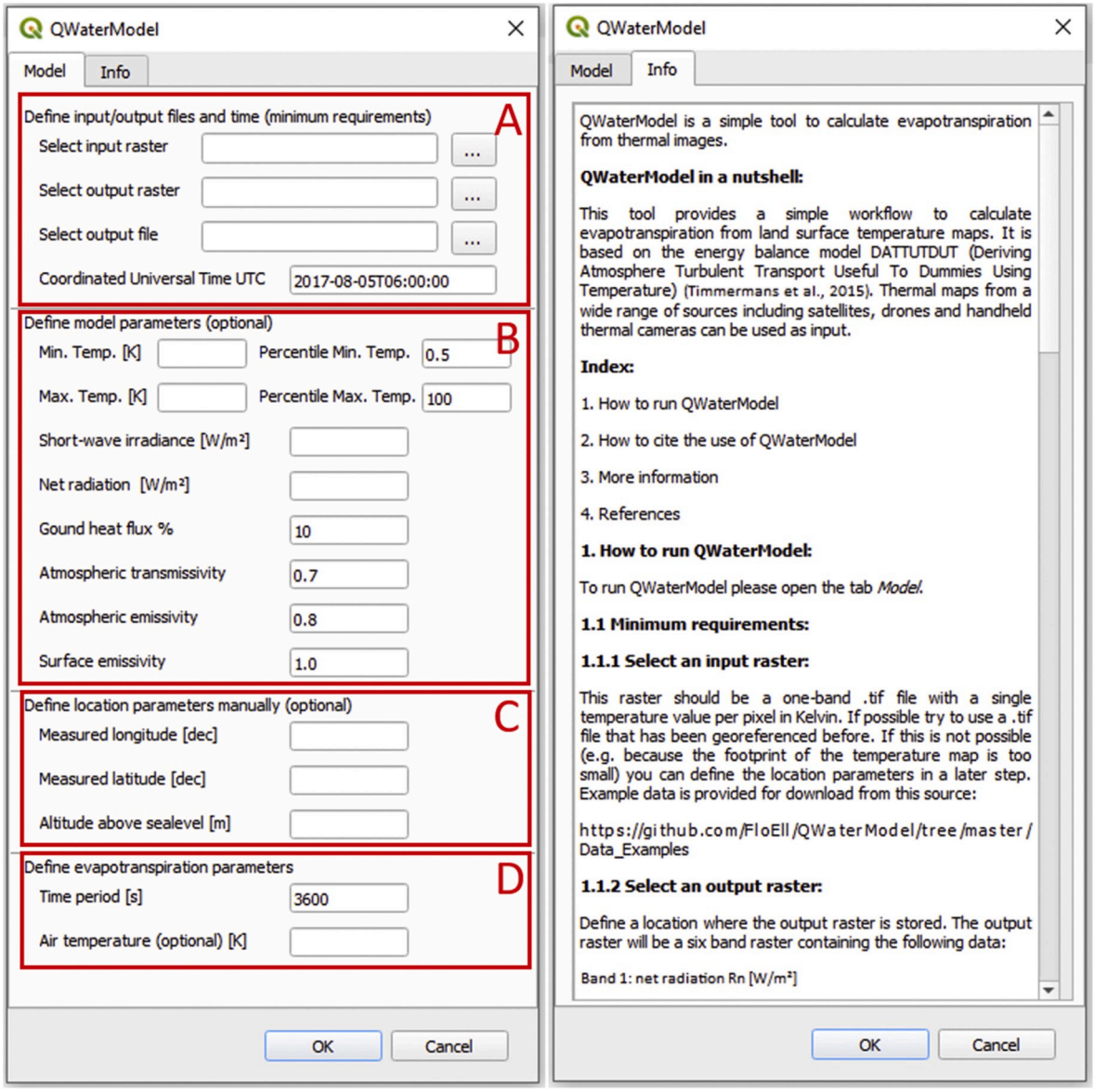

Fig. 1. Both tabs of the graphical user interface (GUI) of the plugin version 1.0 with the 'Model'-tab input boxes highlighted in red.

ET predictions from the plugin with simultaneous ET reference measurements with the well-established eddy covariance method.

2. Methods

2.1. Software design

To facilitate the use of energy balance modeling for ET estimation for a broad audience, we chose QGIS3 (QGIS Development Team, 2020) as a platform. QGIS is a free and open source geographic information system that provides a versatile environment for work flows with spatial data such as LST maps. It offers subsystems for data input and management, analysis, easy visualization of spatial data, has a large community of developers and is supported by most operating systems (Bhatt et al., 2014; Criollo et al., 2019). The use of QGIS is frequently taught in scientific institutions and its functionality can be extended with a large variety of available plugins. For example, the WET (Water Ecosystems Tool) plugin (Nielsen et al., 2017) provides easy access to complex watershed modeling. To our knowledge, no such easy-to-use plugins exist in the QGIS environment for instantaneous flux modeling or ET prediction. The presented plugin, QWaterModel, was developed to fill this gap. It is based on the energy balance model DATTUTDUT (Deriving Atmosphere Turbulent Transport Useful To Dummies Using Temperature) (Timmermans et al., 2015), which uses LST maps as main input and, except for time and location of the LST recording, requires no further input of ancillary data. In the original DATTUTDUT model the radiation budget is simply modelled from a set of parameters and sun-earth geometrics (Timmermans et al., 2015). This approach works well for cloud-free conditions. For a broader usability under conditions of cloudy skies and high relative air humidity we extended this original model concept, giving the user the possibility to configure model parameters according to in-situ field measurements. The radiation budget can be complemented by measurements of short-wave irradiance or net radiation at the study sites via manual input. The DATTUTDUT model has successfully been tested for a broad range of LST input types, from satellite recorded images (Timmermans et al., 2015) to plane and drone recorded images (Brenner et al., 2018; Xia et al., 2016). The plugin was built using Plugin Builder 3.2.1 (GeoApt, 2019) and Plugin Reloader 0.7.9 (Juriel, 2020). We used Qt Creator 4.11.0 (The Qt Company, 2020) to develop the graphical user interface (GUI) and Python 3.8 with the QGIS3/Python standard libraries (gdal, math, numpy, datetime and os) for the associated functionality.

Detailed installation instructions and the source code can be found on: github.com/FloEll/QWaterModel/blob/master/README.md.

2.2. Application and testing

To test the plugin, we used data recorded in a mature monoculture oil palm (*Elaeis guineensis* Jacq.) plantation located in the lowlands of Sumatra (Jambi province, Indonesia, 103.3914411 E, −1.6929879 N, 76 m a.s.l., see Meijide et al. (2017) for further details). We exemplarily use LST recordings from two independent sources (drone and handheld camera) to test the QWaterModel plugin against eddy covariance reference measurements:

1. Images recorded with an octocopter drone (MK EASY Okto V3; HiSystems, Germany) equipped with a radiometric thermal camera FLIR Tau 2 640 (FLIR Systems, USA) attached to a TeAx Thermocapture module (TeAx Technology, Germany). The data have a spatial resolution of 0.2 m and cover a footprint of 0.8 ha and are thus suitable for tree-scale to stand-scale assessments of ET. 13 images from 09:00 to 15:00 h local time on 7th of August 2017 were recorded in 30 min intervals.
2. Images taken from a tower at 10 m above the canopy with a handheld Fluke ti100 thermal camera (Fluke Systems, USA). The data have an approx. spatial resolution of 0.06 m and a footprint of 0.006 ha and are thus suitable for leaf to canopy assessments of ET. 5 images from 11:00 to 15:00 h on 7th of August 2017 were taken in 60 min intervals.

Data are provided for download at: *github.com/FloEll/QWaterModel/tree/master/Data_Examples*

We did not include satellite images into this study since this was already included in the original DATTUTDUT model study (Timmermans et al., 2015). In addition, satellite (Landsat 7 and 8) recorded LST maps for our study region contain a very high cloud cover fraction (for 2017: min. 23%, mean 72%, max. 100%). Our study thus focuses on drone and handheld thermal camera acquired images.

A widely accepted ground-based reference method for ET assessments is the eddy covariance method, which provides measurements of ET at the stand-scale. Eddy covariance data at the oil palm site was recorded, filtered and processed according to the methodology described in Meijide et al. (2017). Because the energy-balance model used in the plugin assumes full energy balance closure, eddy covariance data was processed using the Bowen ratio closure method (Pan et al., 2017; Twine et al., 2000). Horizontal energy flows or incomplete energy balance closure might introduce certain errors to this reference method (Loescher et al., 2006). To derive ET from latent heat fluxes, latent heat of vaporization was calculated using in-situ air temperature measurements for eddy covariance measurements and the lowest pixel temperatures from the LST maps for the plugin estimates following the methodology described in Timmermans et al. (2015).

3. Results

3.1. Software implementation results

The QWaterModel plugin can be installed from the official QGIS3 python plugin repository. The plugin GUI consists of a main window with four different input sections (A, B, C, D, Fig. 1) and an information window, which are both organized using tabs. In the main window, section A contains the inputs that are essential for the plugin to work with in a minimal data approach: a thermal image with temperatures in Kelvin (e.g. from satellite, drone or handheld camera), the definition of an output raster and an output file where key statistics will be summarized, and the coordinated universal time (UTC) when the picture was taken. Providing information in boxes B, C and D is optional, but may improve the quality of the ET estimates. The default values that are visible in the input fields of box B are taken from Timmermans et al. (2015) and can be adjusted if more local data are available from field measurements or previous studies. The info tab offers detailed information on input, output and usage of the plugin. The plugin outputs a raster with 6 bands (net radiation Rn [W m^{-2}], latent heat flux LE [W m^{-2}], sensible heat flux H [W m^{-2}], ground heat flux G [W m^{-2}], evaporative fraction EF in [%] and evapotranspiration ET [mm/time period]). Input raster details and output statistics are stored in a.csv file.

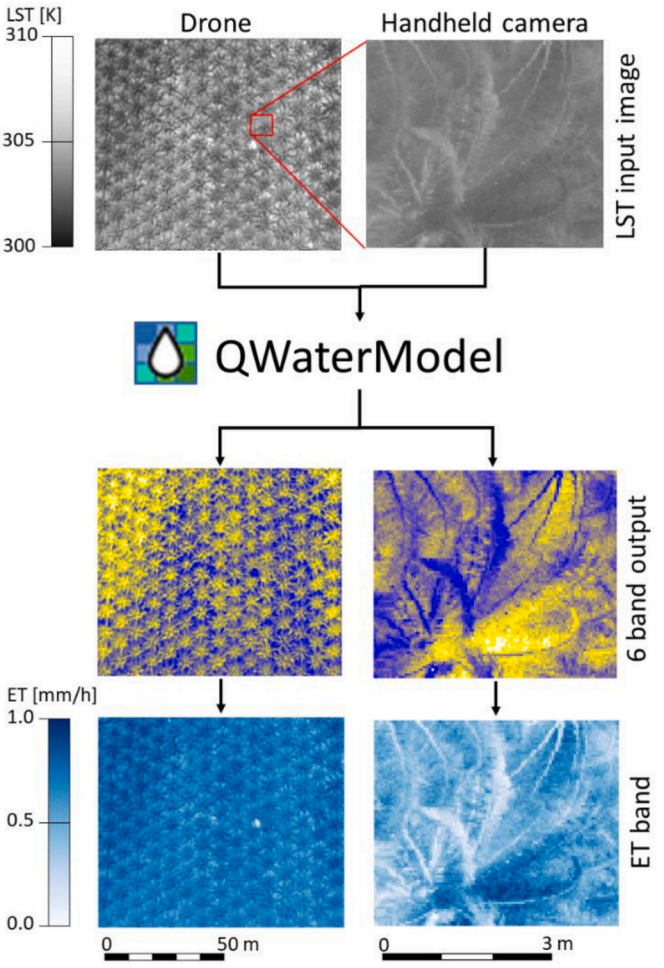

Fig. 2. The ET modelling workflow with input and output examples. The input files are one-layer.tif files where each pixel contains a temperature value in Kelvin. The output files are raster files with 6 bands of which the ET estimates are contained in the 6th band, which is presented separately in the lower panels. ET was extracted from the 6-band output raster using the Rearrange Bands tool from the Processing Toolbox in QGIS 3.10.

Fig. 2 shows a workflow example with LST data from different sources, i.e. recorded from drone and handheld thermal camera and the corresponding output.

3.2. Software experimental testing results

Land surface temperatures differed with the time of recording. Thermal variability was high in both drone and handheld camera

Table 1
Input key-values of land surface temperatures from both sources.

Temperatures	Drone (13 maps)	Handheld camera (5 maps)
Mean Temp. [K]	298.3–305.5	300.8–308.3
Minimum Temp. [K]	297.2–303.0	299.6–305.5
Maximum Temp. [K]	301.2–325.1	302.4–317.0

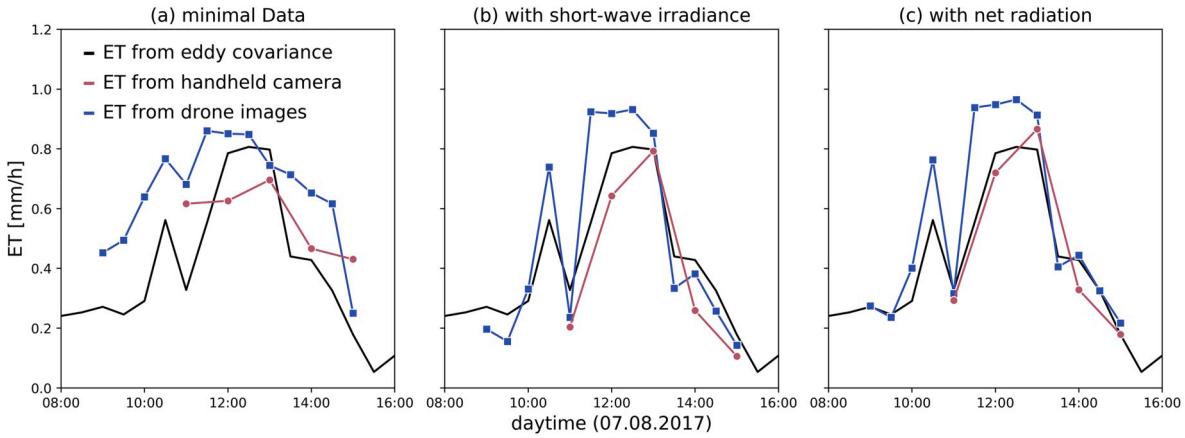

Fig. 3. Temporal comparison of measured reference ET (eddy covariance) and estimated ET from different LST sources during the course of a day.

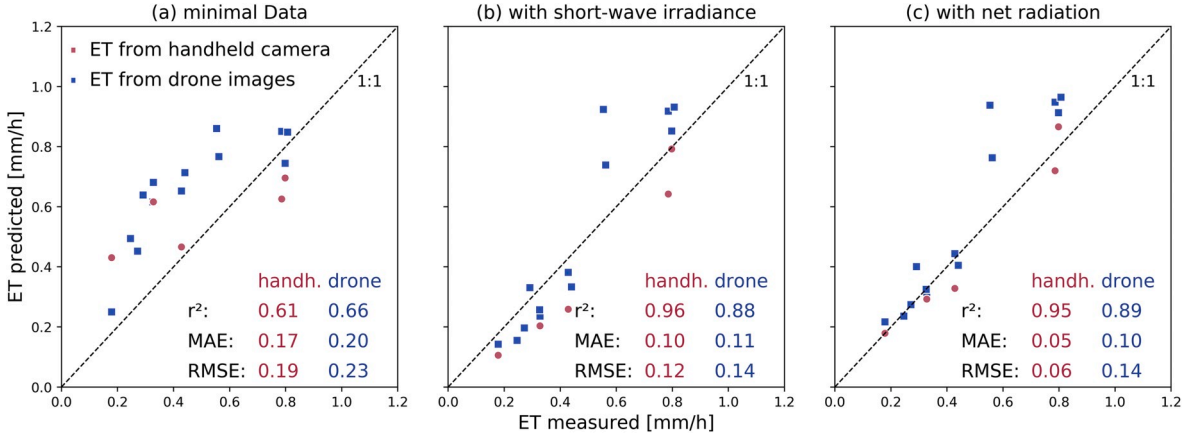

Fig. 4. Comparison of measured reference ET (eddy covariance) and estimated ET from different LST sources; metrics on the respective relationships are provided in Table 2.

Table 2
Key metrics of linear regressions between in-situ measurements and model output for different data input options (a-c) and recording methods (handheld thermal camera and drone).

Metrics	(a) minimal data		(b) with short wave irradiance		(c) with net radiation	
	handheld	drone	handheld	drone	handheld	drone
r^2	0.61	0.66	0.96	0.88	0.95	0.89
MAE	0.17	0.2	0.1	0.11	0.05	0.1
RMSE	0.19	0.23	0.12	0.14	0.06	0.14

obtained maps (Table 1). To compare the ET estimates from drone and handheld thermal camera maps with a measured reference, we plotted them against the daily course of eddy covariance derived ET values (Fig. 3) and into a scatterplot comparing measurements and predictions of ET (Fig. 4).

Applying the energy balance model in its original version with minimal data input resulted in overestimations of ET during the morning and afternoon hours, but in acceptable estimates around noon (Fig. 3a). Errors were smaller for the estimates based on handheld camera pictures than on drone recordings (Table 2). More precise results were achieved by adding measured short-wave irradiance (Fig. 3b) or net radiation measurements (Fig. 3c) to the model inputs, i.e. ET estimates closely follow the reference method if additional radiation data is supplied. The handheld thermal camera maps generally produce slightly more congruent results with the eddy covariance measurements than drone maps; therein, around noon ET estimates from drone maps are slightly higher than eddy covariance ET measurements. In the minimal data approach, ET predictions are most congruent with eddy covariance measurements when ET is high (Fig. 4a), while in contrast predictions are most congruent at low ET when measurements of short-wave irradiance or net radiation are used in the model (Fig. 4b and c). Congruence generally increases with increasing measurement-based input; errors are thus smallest for models computed with directly measured net radiation (Table 2).

4. Discussion and conclusions

The QWaterModel plugin is an easy-to-use open-source tool for predicting evapotranspiration from land surface temperatures. It is aimed at applications in ecology, bioclimatology and land-use science, but is also useful for a broader utilization including hydrological and ecosystem management. It offers a link between science and practical application of energy balance modelling for ET prediction. Meeting our objectives, a variety of LST data from very different sources and spatial extends can be used as input and complementary data input requirements were kept at a minimum level. The case study showed that images taken at the same time but with different camera setups (drone and handheld) result in comparable results for ET estimates and show high congruence with reference eddy covariance measurements. Because in the minimal data approach the radiation budget is calculated from sun-earth geometry, clouds and relative humidity or haze are not considered. This explains the overestimation of ET in the morning and

afternoon hours (Fig. 3a). In-situ measurements of short-wave irradiance or net radiation significantly improved the ET estimates (Fig. 3b and c). Similar observations were made in other studies e.g. on European grasslands where additional short-wave irradiance measurements improved the overall accuracy of the DATTUTDUT model (Brenner et al., 2018). A method comparison of the DATTUTDUT model with the eddy covariance method over varying weather conditions and day times showed the general applicability of this approach in the tropics and suggested no difference between drone-based and eddy covariance method for certain configurations (Ellsäßer et al., submitted). However, even when using measured short-wave or net radiation, ET estimates based on drone recorded LST data showed overestimations around noon, which did not occur in the estimates based on handheld images. A possible reason is the presence of artefacts (e.g. roofs, cars, rocks) in the drone images, which have a much larger footprint than the handheld images. Temperatures on such non-canopy components can differ greatly from surface temperatures of vegetation, and these temperature outliers have a strong effect on the quality of predictions. This was also observed in a study with big temperature differences conducted in vineyards (Xia et al., 2016). A potential solution would be to manually exclude known artefacts from the images before analysis or to manually define minimal and maximal temperatures in the GUI of the plugin. Unfortunately, no matching satellite images were available for the time and date when drone and handheld camera maps were recorded therefore further analyses are not performed in this study. This should be followed up upon in future studies, even though a major restriction in our study region is that satellite images are generally hard to acquire since a considerable cloud cover is present on most days of the year. A further challenge is the fixed overpass time of satellites, which is often not around noon and therefore not ideal for ET derivation (Delogu et al., 2012). To overcome these limitations, complementary ET methods from planes, drones and handheld or fixed thermal cameras can potentially be calibrated against simultaneously acquired satellite images (e.g. using QWaterModel) and then be applied to increase temporal and spatial coverage.

The scatterplots reveal a gap between lower and higher ET estimates (Fig. 4b and c). This gap and its absence in the ET estimates based on modelled Rn in Fig. 4a demonstrates the effects of clouds on prediction accuracy. If clouds are present, and measurements of short-wave irradiance or net radiation can represent this adequately in the model, ET estimates are clearly lower than with the Rn modelling approach.

Future improvements of the software could include a referencing tool that links ground measurements of hot and cold surfaces with LST data. This would allow for a simple radiometric correction of LST images and maps. To make the plugin applicable to the needs of a broader range of users, upcoming versions could further include other LST map-based indices such as the CWSI (crop water stress index) (Bian et al., 2019; Idso et al., 1981; Jones, 2014). We appreciate all user input and ideas to further develop the plugin and encourage to modify the plugin for other ET related applications or to report bugs via our bug tracker. In the present study, the software was only tested at one site, a commercial monoculture oil palm plantation in lowland Sumatra. We strongly encourage the testing and use of the software in other climatic regions and on other crop and ecosystem types for further validation.

We provide the source code for the plugin and plan to consistently add more functionality to the QWaterModel.

5. Software availability

Name of Software: QWaterModel.
Software version: 1.0.
Developers: Florian Ellsäßer;
Software license: GNU - General Public License;
Contact Address: Tropical Silviculture and Forest Ecology, University of Göttingen, Büsgenweg 1, 37077 Göttingen, Germany.
Email: fellsae@gwdg.de.

Availability: plugins.qgis.org/plugins/qwatermodel github.com/FloEll/QWaterModel.

Declaration of competing interest

The authors declare that they have no known competing financial interests or personal relationships that could have appeared to influence the work reported in this paper.

Acknowledgements

This study was funded by the Deutsche Forschungsgemeinschaft (DFG, German Research Foundation) – project number 192626868 – SFB 990 (subprojects A02 and A03) and the Ministry of Research, Technology and Higher Education (Ristekdikti) Indonesia. We thank Ristekdikti for providing the research permit for field work (No. 28/EXT/SIP/FRP/E5/Dit.KI/VII/2017). We thank our field assistant Zulfi Kamal for his support and technician Edgar Tunsch for taking canopy pictures. We also thank Perseroan Terbatas Perkebunan Nusantara VI, Batang Hari Unit (PTPN6) for giving us permission to conduct our research at the oil palm plantation. Thanks to all 'EFForTS' colleagues and friends in Indonesia, Germany, and around the world.

Appendix A. Supplementary data

Supplementary data to this article can be found online at https://doi.org/10.1016/j.envsoft.2020.104739.

References

Allen, R.G., Pereira, L.S., Raes, D., Smith, M., 1998. Crop Evapotranspiration - Guidelines for Computing Crop Water Requirements - FAO Irrigation and Drainage Paper 56. FAO, Rome.
Bhatt, G., Kumar, M., Duffy, C.J., 2014. A tightly coupled GIS and distributed hydrologic modeling framework. Environ. Model. Software 62, 70–84. https://doi.org/10.1016/j.envsoft.2014.08.003.
Bian, J., Zhang, Z., Chen, J., Chen, H., Cui, C., Li, X., Chen, S., Fu, Q., 2019. Simplified evaluation of cotton water stress using high resolution unmanned aerial vehicle thermal imagery. Rem. Sens. 11, 267. https://doi.org/10.3390/rs11030267.
Brenner, C., Zeeman, M., Bernhardt, M., Schulz, K., 2018. Estimation of evapotranspiration of temperate grassland based on high-resolution thermal and visible range imagery from unmanned aerial systems. Int. J. Rem. Sens. 39, 5141–5174. https://doi.org/10.1080/01431161.2018.1471550.
Criollo, R., Velasco, V., Nardi, A., Manuel de Vries, L., Riera, C., Scheiber, L., Jurado, A., Brouyère, S., Pujades, E., Rossetto, R., Vázquez-Suñé, E., 2019. AkvaGIS: an open source tool for water quantity and quality management. Comput. Geosci. 127, 123–132. https://doi.org/10.1016/j.cageo.2018.10.012.
Delogu, E., Boulet, G., Olioso, A., Coudert, B., Chirouze, J., Ceschia, E., Le Dantec, V., Marloie, O., Chehbouni, G., Lagouarde, J.-P., 2012. Reconstruction of temporal variations of evapotranspiration using instantaneous estimates at the time of satellite overpass. Hydrol. Earth Syst. Sci. 16, 2995–3010. https://doi.org/10.5194/hess-16-2995-2012.
Ellsäßer, F., Stiegler, C., Röll, A., June, T., Hendrayanto, Knohl, A., Hölscher, D., submitted. Predicting evapotranspiration from drone-based thermography – a method comparison in a tropical oil palm plantation. Biogeosciences.
Fisher, J.B., Melton, F., Middleton, E., Hain, C., Anderson, M., Allen, R., McCabe, M.F., Hook, S., Baldocchi, D., Townsend, P.A., Kilic, A., Tu, K., Miralles, D.D., Perret, J., Lagouarde, J.-P., Waliser, D., Purdy, A.J., French, A., Schimel, D., Famiglietti, J.S., Stephens, G., Wood, E.F., 2017. The future of evapotranspiration: global requirements for ecosystem functioning, carbon and climate feedbacks, agricultural management, and water resources: the future of evapotranspiration. Water Resour. Res. 53, 2618–2626. https://doi.org/10.1002/2016WR020175.
GeoApt, LLC. https://g-sherman.github.io/Qgis-Plugin-Builder/.
Hoffmann, H., Nieto, H., Jensen, R., Guzinski, R., Zarco-Tejada, P., Friborg, T., 2016. Estimating evaporation with thermal UAV data and two-source energy balance models. Hydrol. Earth Syst. Sci. 20, 697–713. https://doi.org/10.5194/hess-20-697-2016.
Idso, S.B., Jackson, R.D., Pinter, P.J., Reginato, R.J., Hatfield, J.L., 1981. Normalizing the stress-degree-day parameter for environmental variability. Agric. Meteorol. 24, 45–55. https://doi.org/10.1016/0002-1571(81)90032-7.
Jones, H.G., 2014. Plants and Microclimate: a Quantitative Approach to Environmental Plant Physiology, third ed. Cambridge University Press, Cambridge ; New York.
Juriel, B.. https://github.com/borysiasty/plugin_reloader.
Kaushal, S., Gold, A., Mayer, P., 2017. Land use, climate, and water resources—global stages of interaction. Water 9, 815. https://doi.org/10.3390/w9100815.
Loescher, H.W., Law, B.E., Mahrt, L., Hollinger, D.Y., Campbell, J., Wofsy, S.C., 2006. Uncertainties in, and interpretation of, carbon flux estimates using the eddy

covariance technique. J. Geophys. Res. 111, D21S90. https://doi.org/10.1029/2005JD006932.
Maes, W.H., Steppe, K., 2012. Estimating evapotranspiration and drought stress with ground-based thermal remote sensing in agriculture: a review. J. Exp. Bot. 63, 4671–4712. https://doi.org/10.1093/jxb/ers165.
Meijide, A., Röll, A., Fan, Y., Herbst, M., Niu, F., Tiedemann, F., June, T., Rauf, A., Hölscher, D., Knohl, A., 2017. Controls of water and energy fluxes in oil palm plantations: environmental variables and oil palm age. Agric. For. Meteorol. 239, 71–85. https://doi.org/10.1016/j.agrformet.2017.02.034.
Nielsen, A., Bolding, K., Hu, F., Trolle, D., 2017. An open source QGIS-based workflow for model application and experimentation with aquatic ecosystems. Environ. Model. Software 95, 358–364. https://doi.org/10.1016/j.envsoft.2017.06.032.
Oki, T., Kanae, S., 2006. Global hydrological cycles and world water resources. Am. Assoc. Adv. Sci. 313, 1068–1072. https://doi.org/10.1126/science.1128845.
Pan, X., Liu, Y., Fan, X., Gan, G., 2017. Two energy balance closure approaches: applications and comparisons over an oasis-desert ecotone. J. Arid Land 9, 51–64. https://doi.org/10.1007/s40333-016-0063-2.
QGIS Development Team, 2020. QGIS Geographic Information System. Open Source Geospatial Foundation Project. http://qgis.osgeo.org.
Timmermans, W.J., Kustas, W.P., Andreu, A., 2015. Utility of an automated thermal-based approach for monitoring evapotranspiration. Acta Geophys. 63, 1571–1608. https://doi.org/10.1515/acgeo-2015-0016.
Twine, T.E., Kustas, W.P., Norman, J.M., Cook, D.R., Houser, P.R., Meyers, T.P., Prueger, J.H., Starks, P.J., Wesely, M.L., 2000. Correcting eddy-covariance flux underestimates over a grassland. Agric. For. Meteorol. 103, 279–300. https://doi.org/10.1016/S0168-1923(00)00123-4.
Xia, T., Kustas, W.P., Anderson, M.C., Alfieri, J.G., Gao, F., McKee, L., Prueger, J.H., Geli, H.M.E., Neale, C.M.U., Sanchez, L., Alsina, M.M., Wang, Z., 2016. Mapping evapotranspiration with high-resolution aircraft imagery over vineyards using one- and two-source modeling schemes. Hydrol. Earth Syst. Sci. 20, 1523–1545. https://doi.org/10.5194/hess-20-1523-2016.
Ziegler, A.D., Sheffield, J., Maurer, E.P., Nijssen, B., Wood, E.F., Lettenmaier, D.P., 2003. Detection of intensification in global- and continental-scale hydrological cycles: temporal scale of evaluation. J. Clim. 16, 13.
The Qt Company (2020). Qt Creator 4.11.0. https://www.qt.io/.